

Temperature independence of the spin-injection efficiency of a MgO-based tunnel spin injector

G. Salis^{a)}

IBM Research, Zurich Research Laboratory, Säumerstrasse 4, 8803 Rüschlikon, Switzerland

R. Wang,^{b)} X. Jiang, R. M. Shelby, and S. S. P. Parkin

IBM Research, Almaden Research Center, San Jose, California 95120

S. R. Bank and J. S. Harris

Solid State and Photonics Laboratory, Stanford University, Stanford, California 94305

(Received 7 September 2005; accepted 13 November 2005; published online 20 December 2005)

The spin polarization of electrons injected into GaAs from a CoFe/MgO(100) tunnel spin injector is inferred from the circular polarization of light emitted from a GaAs-based quantum well (QW) detector. The circular polarization strongly depends on the spin and electron hole recombination lifetimes in the QW. Using time-resolved optical techniques, we show that these lifetimes are highly temperature dependent. A peak in the charge lifetime versus temperature is likely responsible for the previously observed dip in the electroluminescence polarization. Evidence for a temperature-independent spin injection efficiency of $\sim 70\%$ from 10 K to room temperature is found. © 2005 American Institute of Physics. [DOI: 10.1063/1.2149369]

Spin injection from ferromagnetic contacts into semiconductors is a key ingredient for spintronic applications. Recently, spin injection from various ferromagnetic materials into GaAs-based semiconductors has been reported.¹⁻⁷ In these experiments, the spin polarization in the semiconductor is detected optically by measuring the degree of circular polarization P_{EL} of the electroluminescence (EL) emitted from recombining electrons in a semiconductor quantum well (QW). In general, P_{EL} depends in a complex way on bias and temperature T .⁶⁻⁸ Apart from a possible loss of spin polarization as the electron travels from the ferromagnetic contact to the QW, the spin and charge decay in the QW detector plays a significant role in the magnitude of the P_{EL} .

In this letter, we systematically study both spin and charge lifetimes in QWs that serve as spin detectors for spin injection from CoFe/Mg(100) contacts into GaAs. Lifetimes are determined from time-resolved Kerr rotation (KR) and time-resolved differential reflectivity (DR) measurements. The samples investigated exhibit a P_{EL} up to 50% with a pronounced dip in $P_{\text{EL}}(T)$ whose position in T depends on the QW confinement. We show experimentally that this dip derives mainly from a peak in the charge recombination time τ . With longer τ , more of the injected electron spins relax before recombining with holes. Accounting for the resulting reduction in P_{EL} , we find evidence of an injected spin polarization of $\sim 70\%$ that shows only a slight dependence on T up to room temperature.

In this letter, the samples were prepared in a two-step process as described in Ref. 6. The semiconductor QW heterostructure used for detection was grown by molecular beam epitaxy on a p -doped GaAs substrate ($p \sim 1 \times 10^{19} \text{ cm}^{-3}$) with the following structure: 580 nm p -doped $\text{Al}_x\text{Ga}_{1-x}\text{As}$,⁹ 75 nm $\text{Al}_x\text{Ga}_{1-x}\text{As}$, 10 nm GaAs, 15 nm $\text{Al}_x\text{Ga}_{1-x}\text{As}$, 100 nm p -doped $\text{Al}_x\text{Ga}_{1-x}\text{As}$,

($p \sim 1 \times 10^{17} \text{ cm}^{-3}$), and finally a 5-nm-thick undoped GaAs top layer to protect the AlGaAs layers from oxidation during processing. For these experiments, sample 1 was grown with a 16% Al-doped barrier ($x=0.16$) and sample 2 was grown with a 8% Al barrier ($x=0.08$). Magnetron sputtering was then used to deposit ~ 3 -nm-thick MgO tunnel barriers followed by 5-nm-thick $\text{Co}_{70}\text{Fe}_{30}$ top electrodes. Finally, a 5-nm-thick Ta capping layer was added to prevent oxidation of the CoFe.

For the measurement of spin and charge lifetimes, the samples were placed in an optical cold-finger cryostat. A circularly polarized pump and a linearly polarized probe beam from a mode-locked Ti:sapphire laser were focused to overlapping spots on the CoFe/MgO injector. The angle of incidence of both beams was about 5° to the sample normal. The diameter of the probe beam was $\sim 20 \mu\text{m}$, while the pump beam was slightly broader. The 2 ps probe-beam pulses were delayed with respect to the pump pulses by a time Δt between -150 and 3000 ps. The circularly polarized pump pulses were tuned to the heavy-hole absorption peak of the QW and thus were expected to create $\sim 100\%$ spin-polarized electron-hole pairs in the QW. Owing to the magneto-optical KR effect, the polarization axis of the probe beam reflected off the sample was rotated by an angle proportional to the electron spin polarization along the probe-beam direction. Using lock-in techniques, only the pump-induced KR was measured in a balanced bridge setup, thus eliminating KR from the ferromagnetic electrode. Pump-induced changes of the reflected probe intensity were monitored simultaneously using additional lock-in amplifiers. In order to make the conditions in the QW as close as possible to the ones when measuring P_{EL} (described in Ref. 6), a magnetic field B along the sample normal as well as an electric bias between the CoFe and an ohmic contact on the backside of the p -doped GaAs substrate were applied. The negative contact was on the CoFe side.

Figure 1 shows traces of time-resolved KR and DR for sample 1 at $T=25$ and 125 K, $B=0.8$ T and an applied bias

^{a)} Author to whom correspondence should be addressed; electronic mail: gsa@zurich.ibm.com

^{b)} Also at: Solid State and Photonics Laboratory, Stanford University, Stanford, California 94305.

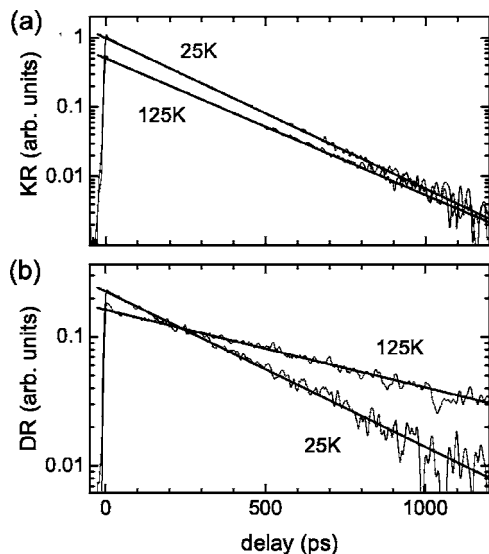


FIG. 1. Time-resolved Kerr rotation (a) and differential reflectivity (b) for the QW with 16% Al measured at 25 and 125 K, $B=0.8$ T and a bias of 2.0 V. The exponential decay of the KR signal is given by both spin decay and charge recombination, whereas the time evolution of the differential reflectivity is affected only by charge recombination. Exponential fits appear as straight lines. From these measurements, the spin lifetime τ_s and the charge recombination time τ are determined.

of 2.0 V. The data are obtained with an average pump power of $80 \mu\text{W}$ and a probe power of $8 \mu\text{W}$. The KR data in Fig. 1 is the difference between two sets of measurements using pump beams with opposite circular polarization. Both KR and DR decay exponentially, but with different decay constants. The decay in DR is due to charge recombination,¹⁰ and an exponential fit yields the charge recombination time τ . The decay time T_s of the KR signal is given by both τ and the spin lifetime τ_s through $T_s^{-1} = \tau_s^{-1} + \tau^{-1}$, because the KR angle is proportional to both the spin polarization and the number of electrons in the QW. For the fits shown in Fig. 1, we obtain $T_s=200$ (220) ps and $\tau=360$ (722) ps at $T=25$ (125) K.

The decay times τ and T_s are measured between 10 and 300 K for sample 1, and are presented in Fig. 2(a), together with τ_s . Open and closed symbols are for $B=0$ and 0.8 T, respectively. The charge-recombination time τ increases from ~ 300 ps at 10 K to more than 700 ps at 125 K. At higher temperatures, τ decreases and reaches ~ 150 ps at room temperature. Such a nonmonotonic behavior has been observed previously in Refs. 10–12, and is explained by an interplay of a radiative recombination time that increases with T ¹³ and a nonradiative lifetime that decreases with T . The error bars [as shown for the data points at 175 and 290 K in Fig. 2(a)] arise from a variation of the measured lifetime with the optical wavelength, an uncertainty of the exponential fit due to an offset in the time-resolved reflectivity measurements, and device variations across the wafer. Taking the estimated error into account, we do not observe a significant B dependence of τ for sample 1 up to 0.8 T. On the other hand, τ_s clearly shows an increase with B of about 5%–20% at 0.8 T, which is larger than the estimated error in T_s of about 5 ps.

At the time of recombination in the QW, the average injected spin polarization is reduced by a factor $\rho = \tau_s / (\tau_s + \tau) = T_s / \tau$.¹⁴ For example, $0.7 \cdot \rho$ represents the EL polarization one would observe from the QW if the CoFe/MgO con-

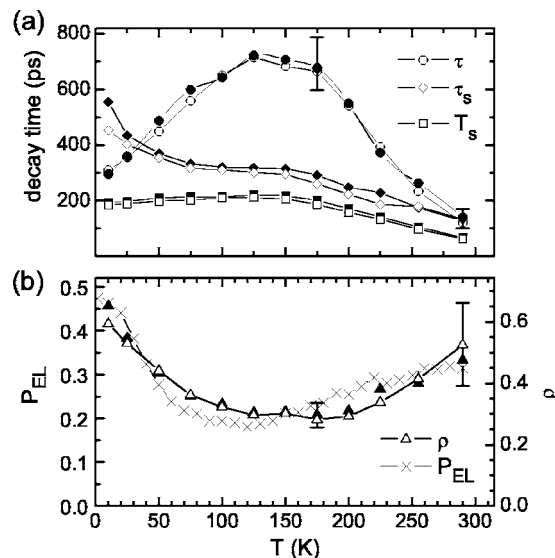


FIG. 2. (a) Measured τ (circles), T_s (squares) and τ_s (diamonds) vs T for the sample with 16% Al and a bias of 2.0 V. The curve of τ_s exhibits a monotonic decrease with T , whereas τ peaks at ~ 125 K owing to the onset of nonradiative recombination. (b) Spin detector efficiency $\rho = T_s / \tau$ (triangles) as obtained from (a), together with measured P_{EL} (crosses). The scale for ρ is chosen such that $P_{\text{EL}}=0.7$ coincides with $\rho=1$, i.e., a match of the two curves corresponds to 70% spin injection efficiency. Open and closed symbols are for $B=0$ and 0.8 T, respectively.

tact injects 70% spin-polarized electrons. Figure 2(b) shows ρ for sample 1 together with P_{EL} ⁶ measured on a sample from the same wafer at a bias of 2.0 V. Open symbols represent data obtained at zero field, whereas closed symbols were obtained at $B=0.8$ T. Qualitatively, the temperature behavior of ρ is very similar to that seen in P_{EL} , showing a characteristic dip that can be related to the observed peak in τ . The data in Fig. 2 indicate a spin-injection efficiency of $\sim 70\%$ up to room temperature.

Note that the $P_{\text{EL}}(T)$ minimum appears slightly displaced towards smaller T relative to $\rho(T)$. Such deviations could arise from the different experimental conditions used for the time-resolved optical studies. The optical excitation with pump pulses leads to a modification of the band profile that is different than for electrical injection alone. Without optical excitation, injected electrons recombine with unpolarized holes from the p -doped substrate, whereas optical pumping directly provides heavy holes for recombination, which possibly modifies τ as well as τ_s . We have taken care to minimize this effect by using a pump power that is low enough to eliminate the data dependence on pump power. Also, τ and T_s presented in Fig. 2 are obtained at 0 and 0.8 T, while P_{EL} is the polarization measured when the CoFe moments are fully polarized out of plane after linear subtraction of a B -dependent background signal.⁶ In our experimental configuration, it was not possible to apply larger magnetic fields than 0.8 T.

In a shallower QW sample with an Al concentration in the barrier of 8% (sample 2), the peak in τ is displaced towards lower T , as seen from Fig. 3(a). This result is in agreement with results from Ref. 12 as well as with experiments on narrow QWs,¹¹ where, due to the smaller QW confinement, the onset of nonradiative decay occurs at lower T owing to thermally activated carrier escape. Because of the weak confinement of carriers in sample 2, EL can only be observed up to 100 K. Also included in Fig. 3(a) are data

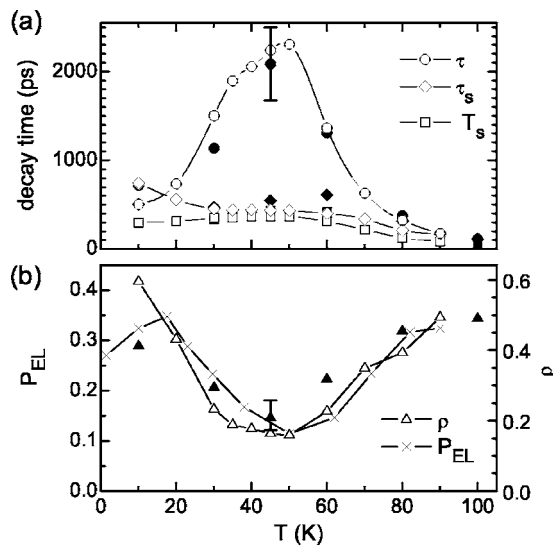


FIG. 3. (a) Measured τ (circles), τ_s (diamonds) and T_s (squares) vs T for the sample with 8% Al and a bias of 1.9 V. Open and closed symbols are for $B=0$ and 0.8 T, respectively. In (b), ρ (triangles) is compared to measured P_{EL} (crosses). Again, the scale for ρ is plotted to represent 70% injected spin polarization.

obtained at $B=0.8$ T (filled symbols). At $T=10$ K, τ increases with B , whereas it decreases slightly at higher T , but this trend is smaller than the estimated error (see error bar at 45 K). The KR decay time T_s increases by about 20%–30% with B for $T>30$ K.

In Fig. 3(b) the resulting ρ of sample 2 is compared with P_{EL} measured at a bias of 1.9 V. Once again, the nonmonotonic temperature dependence of ρ qualitatively matches the behavior of P_{EL} , and the data indicate a spin-injection efficiency of $\sim 70\%$ over the temperature range measured. The increase of ρ with the applied field for $T>30$ K is due to a corresponding increase of τ_s , which can be explained with magnetic field suppression of D'yakonov–Perel spin relaxation for free electrons.¹⁵ In our samples, we do not observe a significant increase of τ_s with T for $T>70$ K, contrary to what has been suggested to be responsible for an increase of P_{EL} with T .^{6,7}

In conclusion, time-resolved Kerr rotation, differential reflectivity, and electrical spin injection experiments per-

formed on two different GaAs QW spin detectors suggest that the T dependence of the carrier recombination in the QW is largely responsible for the nonmonotonic temperature dependence of P_{EL} observed in recent spin-injection experiments. While both spin and recombination lifetimes affect P_{EL} vs T , the observed dip in P_{EL} that occurs in both samples is attributed to a corresponding peak in the recombination lifetime in the QW. These results show that the electrical spin injection efficiency from CoFe/MgO spin injectors exhibits a much smaller temperature dependence than the electroluminescence polarization, and indicate a high injection efficiency of $\sim 70\%$ for temperatures from 10 K up to room temperature.

The authors thank R. Allenspach and L. Meier for fruitful discussions, and M. Witzig for technical assistance. This work was supported in part by DARPA.

- ¹R. Fiederling, M. Keim, G. Reuscher, W. Ossau, G. Schmidt, A. Waag, and L. W. Molenkamp, *Nature (London)* **402**, 787 (1999).
- ²Y. Ohno, D. K. Young, B. Beschoten, F. Matsukura, H. Ohno, and D. D. Awschalom, *Nature (London)* **402**, 790 (1999).
- ³H. J. Zhu, M. Ramsteiner, H. Kostial, M. Wassermeier, H.-P. Schönherr, and K. H. Ploog, *Phys. Rev. Lett.* **87**, 016601 (2001).
- ⁴A. T. Hanbicki, B. T. Jonker, G. Itskos, G. Kioseoglou, and A. Petrou, *Appl. Phys. Lett.* **80**, 1240 (2002).
- ⁵V. F. Motsnyi, J. DeBoeck, J. Das, W. V. Roy, and G. Borghs, *Appl. Phys. Lett.* **81**, 265 (2002).
- ⁶X. Jiang, R. Wang, R. M. Shelby, R. M. Macfarlane, S. R. Bank, J. S. Harris, and S. S. P. Parkin, *Phys. Rev. Lett.* **94**, 056601 (2005).
- ⁷C. Adelman, X. Lou, J. Strand, C. J. Palmström, and P. A. Crowell, *Phys. Rev. B* **71**, 121301 (2005).
- ⁸X. Y. Dong, C. Adelman, J. Q. Xie, C. J. Palmström, X. Lou, J. Strand, P. A. Crowell, J.-P. Barnes, and A. K. Petford-Long, *Appl. Phys. Lett.* **86**, 102107 (2005).
- ⁹Beryllium p -type dopant is graded from $1 \times 10^{19} \text{ cm}^{-3}$ down to $1 \times 10^{15} \text{ cm}^{-3}$ in this layer.
- ¹⁰F. Fernández-Alonso, M. Righini, A. Franco, and S. Selci, *Phys. Rev. B* **67**, 165328 (2003).
- ¹¹M. Gurioli, A. Vinattieri, M. Colocci, C. Deparis, J. Massies, G. Neu, A. Bosacchi, and S. Franchi, *Phys. Rev. B* **44**, 3115 (1991).
- ¹²J. Tignon, O. Heller, P. Roussignol, J. Martinez-Pastor, P. Lelong, G. Bastard, R. C. Iotti, L. C. Andreani, V. Thierry-Mieg, and R. Planel, *Phys. Rev. B* **58**, 7076 (1998).
- ¹³J. Feldmann, G. Peter, E. O. Göbel, P. Dawson, K. Moore, C. Foxon, and R. J. Elliott, *Phys. Rev. Lett.* **59**, 2337 (1987).
- ¹⁴S. F. Alvarado and P. Renaud, *Phys. Rev. Lett.* **68**, 1387 (1992).
- ¹⁵*Optical Orientation*, edited by F. Meier and B. P. Zakharchenya (North-Holland, New York, 1984).